# Transport quantum logic gates for trapped ions

D. Leibfried, E. Knill, C. Ospelkaus, and D. J. Wineland
*National Institute of Standards and Technology, 325 Broadway, Boulder, Colorado 80305, USA*
(Received 24 July 2007; published 21 September 2007)

Many efforts are currently underway to build a device capable of large scale quantum information processing (QIP). Whereas QIP has been demonstrated for a few qubits in several systems, many technical difficulties must be overcome in order to construct a large-scale device. In one proposal for large-scale QIP, trapped ions are manipulated by precisely controlled light pulses and moved through and stored in multizone trap arrays. The technical overhead necessary to precisely control both the ion geometrical configurations and the laser interactions is demanding. Here we propose methods that significantly reduce the overhead on laser-beam control for performing single- and multiple-qubit operations on trapped ions. We show how a universal set of operations can be implemented by controlled transport of ions through stationary laser beams. At the same time, each laser beam can be used to perform many operations in parallel, potentially reducing the total laser power necessary to carry out QIP tasks. The overall setup necessary for implementing transport gates is simpler than for gates executed on stationary ions. We also suggest a transport-based two-qubit gate scheme utilizing microfabricated permanent magnets that can be executed without laser light.

DOI: 10.1103/PhysRevA.76.032324 PACS number(s): 03.67.Lx, 32.80.Pj

## I. INTRODUCTION

A number of physical implementations have been proposed for quantum information processing (QIP) [1]. This paper is based on a proposal where trapped atomic ion qubits are to be held in a large trap array [2,3]. Its implementation requires transporting ions between separated zones, precise control of local potentials and, at the same time, precise control of laser-beam pointing, intensity, and pulse shape. These requirements create an imposing overhead of classical control for large trap arrays with multiple interaction zones. Ion transport is accomplished by electronically changing the potentials of individual control electrodes in the trap array [4] and might be realized with on-board complementary metal-oxide semiconductor electronics [5], a technology with a long and very successful track record for scaling. The situation is very different for the optics necessary for laser-beam control: Microfabricated beam-steering optics and electro-optical devices are typically still "one-of-a-kind" designs with only small numbers produced and scalability in the context of QIP still to be demonstrated. This problem is compounded by the wavelengths that are of interest in QIP with trapped ions, which are typically in the near ultraviolet (uv) between 214 nm and 400 nm. In addition, a mature optical fiber technology does not yet exist for this wavelength range. It is anticipated that high laser power will be required in QIP with trapped ions [6], so beam splitters or lossy elements should be used sparingly. At the same time, fault tolerant architectures require implementing parallel operations [7]. Miniaturization of the currently used approach with switched beams, as discussed in [5] (for example), is based on the use of a large number of beam splitters and control elements to achieve both parallel and individual control of many different gate operations. Even if the elements used have little loss (which is currently hard to achieve in the uv), parallel operations would magnify the already demanding power requirements.

The purpose of this paper is to show that precise control of the time-dependent external potentials used to transport ions within a trap array can replace the requirement for precise temporal control of laser-beam intensity in order to implement universal quantum computation. In an architecture based on transport, laser beams can be switched on and off collectively with relaxed requirements on timing and on-off ratios. Such a scenario may also allow for efficient use of one and the same laser beam in many parallel operations, thus achieving parallelism without the need for higher laser power. Under such circumstances it is even conceivable to further enhance the available power in laser beams with optical cavities of modest finesse.

The paper is organized as follows: Section II outlines the basic architecture and QIP primitives necessary for universal quantum computation with the proposed scheme. We concentrate on qubits that are comprised of the hyperfine states of ions, which are manipulated by stimulated two-photon Raman transitions [2], but it is possible to adapt the basic architecture for ion qubits of a different type. Sections III and IV briefly summarize the necessary Raman laser interactions and the spatial dependence of the laser-beam modes used in subsequent sections. Sections V and VI outline the details of one-qubit rotations and two-qubit phase gates implemented by ion transport through laser beams. Section VII discusses how sympathetic cooling can be incorporated and Sec. VIII introduces some possible extensions of the scheme, including a two-qubit gate based on transporting ions over a periodic array of microfabricated permanent magnets, without the need for laser beams. Finally we summarize and offer some conclusions in Sec. IX.

## II. BASIC ARCHITECTURE

The goal of the architecture discussed here is to minimize the requirements on laser-beam steering, pulse shaping and switching as much as possible by utilizing temporal control of potentials applied to the ions in a multizone trap array. Temporal control is already needed for efficient transport, separation, and recombination of ions, so, with refinements,

 

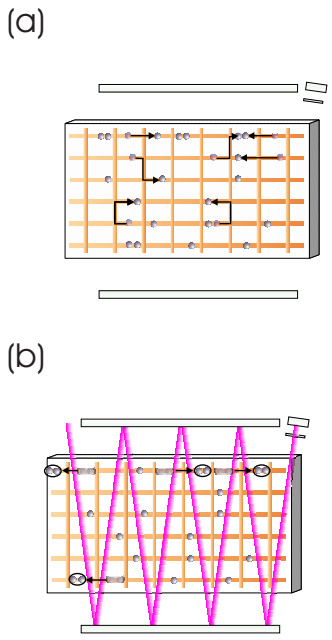


FIG. 1. (Color online) Basic steps for the proposed architecture: (a) The ions carrying the quantum information are arranged into the desired spatial configuration in the trap array while the laser beams are switched off. (b) All laser-beam-assisted operations scheduled after the prearrangement in (a) are carried out. This includes one-qubit rotations, two-qubit gates, and measurements.

we can also employ it for qubit gate operations.

Our proposed architecture is based on a multizone geometry [2,3,5,8–10]. To be specific we consider planar surface electrode trap arrays [11] in the following, but the basic ideas should also work in other types of trap arrays. In this architecture, logic operations are implemented by two basic primitive steps.

(i) The ions carrying the quantum information are arranged into a particular spatial configuration in the trap array while the laser beams are switched off [Fig. 1(a)].

(ii) All laser-beam-assisted operations scheduled for the configuration are implemented after (i) is carried out. The laser beam(s) are collectively switched on, then single-qubit ions or pairs of qubit ions are transported through the laser beams to implement one-qubit rotations, two-qubit gates, and measurements [Fig. 1(b)]. Finally, the laser beams are switched off collectively.

Steps (i) and (ii) are repeated until the computation is finished. In more detail, the control for ion motion in (i) can be accomplished with a few sequential elementary substeps. For example, these substeps could be translations of the potential wells containing an ion or ions in the array and splitting and recombining potential wells to reconfigure ions into different groupings [4,12]. These basic operations are indicated schematically in Fig. 1(a). In addition to these classical means of transport, quantum information can be transported in the array without physically moving the information carriers by teleportation [12–15]. Teleportation could be supported by a backbone of entangled qubits distributed over the whole array before and/or in parallel with the computation. Such an entanglement backbone could also be part of an efficient error correction scheme [16].

After the preconfiguration of qubits in the array, step (ii) is implemented. This step can be broken down into three basic laser-assisted suboperations that we call *transport gates*: single-qubit rotations, two-qubit gates, and measurement. Single-qubit rotations can be initiated by first turning on specific laser beams globally over the entire array. Then, the qubits scheduled for one-qubit rotations are transported through the laser beams in a controlled fashion [see Fig. 1(b)]. Next the beams for two-qubit gates are turned on and the pairs of ions scheduled for two-qubit gates are transported through the beams. Finally, all qubits scheduled for measurement are read out by either turning on a detection beam at their current location or transporting them through a globally switched detection beam. Depending on the exact nature of the detection scheme, all measurements can be done in parallel if position-resolving detectors are used. Alternatively, detection could be accomplished serially with scheduled transports if no (or only limited) position resolution is available. The physical implementation of one-qubit rotations and two-qubit gates is discussed in Secs. V and VI, respectively.

Previously, temporal control of ions' internal states, such as qubit rotations, had to be achieved by individually calibrated, precise switching of laser beams. With transport gates laser beams can be switched on and off globally over the entire trap array while precise individual control is now transferred to the ion motion. This also facilitates the use of one set of laser beams for parallel operations on ions distributed over the trap array, reduces the complexity of optics, and might lead to lower requirements on the total laser power necessary to run processors with a certain number of qubits.

By repetition of (i) and (ii) we can realize one-qubit rotations, two-qubit gates, and measurement between arbitrary qubits in an arbitrary order, which is sufficient for universal quantum computation [17]. Individual operations are then controlled by the motion of ions alone, while the switching of lasers can be implemented with reduced timing precision. This could be of significant practical importance, if active feedback on the lasers to counteract intensity or beam position fluctuations is desired. In the traditional scheme where operations depend on the temporal characteristics of the laser beams, such feedback would have to act on time scales much shorter than that of the laser pulses. In the scheme discussed here, the transport of the ions can be delayed by a suitable amount of time for the feedback to settle. Such a procedure could also alleviate the detrimental effects of other switching imperfections, such as phase chirps in acousto-optic modulators. As a further example of the potential simplification, consider the problem of implementing in parallel a specific rotation on several spatially separated qubits with the same laser beam. If the rotation is implemented by applying a pulse to ions already in place, we require the laser intensity to be the same at the site of each ion, a difficult task, given the general divergence and/or convergence of the laser beams. This problem can be alleviated by controlling the transport of each qubit through the beam separately. Furthermore, since the ions are transported completely through the laser beams, the gate interaction does not change if beams have small pointing instabilities in the plane of the trap array

that change on a time scale long compared to the gate interactions (typically fulfilled for beam-steering time scales in the laboratory). It is therefore sufficient to stabilize the beam pointing in the direction perpendicular to the motion of the ions.

## III. TWO-PHOTON STIMULATED RAMAN INTERACTIONS

In this section we briefly review the basic interactions that play a role in the transport gates discussed later. We assume that we have perfect control of the ion motion in the array; in particular, we assume that we can confine one- or two-qubit ions in one potential well with precisely defined motional frequencies, and we also assume we can translate the well along a predefined trajectory without changing the motional frequencies. We assume that the ions start in and remain in the motional ground state in the accelerating phases at the beginning and end of the transport and that the well is translated with a constant velocity $\mathbf{v}$ relative to the laboratory frame while the ions move through the laser beams. This situation, as viewed from the ions' frame of reference, is equivalent to that of ions in the ground state in a stationary potential well under the influence of temporally controlled laser beams. We can therefore describe one-qubit gates and two-qubit gates with the interaction Hamiltonians that are also appropriate for ions at rest in the laboratory frame. The difference is that, for each operation, the coordinates of the ions are transformed by $\mathbf{r}\rightarrow\mathbf{r}_{\mathrm{lab}}+\mathbf{v}\ t$ with $\mathbf{r}_{\mathrm{lab}}$ a point at rest in the laboratory frame that is taken to coincide with $\mathbf{r}$ at time $t=0$. We assume the qubit state space is spanned by two hyperfine ground states of each ion, formally equivalent to the two states of a spin-$\frac{1}{2}$ magnetic moment in a magnetic field. We therefore label the qubit states $|\uparrow\rangle$ and $|\downarrow\rangle$ and denote their energy difference by $\hbar\omega_0$. We consider stimulated Raman transitions [2,18], implemented with two laser beams with wave vectors $\mathbf{k}_1$ and $\mathbf{k}_2$ and frequencies $\omega_1$ and $\omega_2$. After adiabatic elimination of the off-resonant levels, the effective interactions of one ion with two Raman laser beams can be described in the rotating wave approximation by the Hamiltonian [2,19,20]

$$\begin{aligned} H_I = {} & \hbar\Omega_0 e^{-i([\delta_0-\omega_0]t+\phi)} e^{i\Delta\mathbf{k}\cdot\mathbf{r}}|\uparrow\rangle\langle\downarrow| + \mathrm{H.c.} \\ & + \hbar\Omega_\uparrow e^{-i(\delta_0 t+\phi)} e^{i\Delta\mathbf{k}\cdot\mathbf{r}}|\uparrow\rangle\langle\uparrow| + \mathrm{H.c.} + \hbar\Omega_\downarrow e^{-i(\delta_0 t+\phi)} e^{i\Delta\mathbf{k}\cdot\mathbf{r}}|\downarrow\rangle \\ & \times\langle\downarrow| + \mathrm{H.c.} + \hbar\Delta_\downarrow|\downarrow\rangle\langle\downarrow| + \hbar\Delta_\uparrow|\uparrow\rangle\langle\uparrow|, \end{aligned} \tag{1}$$

where H.c. is the Hermitian conjugate of the previous term, $\hbar$ is Planck's constant divided by $2\pi$, $\delta_0=\omega_1-\omega_2$ is the frequency difference, $\Delta\mathbf{k}=\mathbf{k}_1-\mathbf{k}_2$ is the wave vector difference, and $\phi=\phi_1-\phi_2$ is the phase difference of the two laser fields at $\mathbf{r}=0$. The above expression breaks the total interaction down into three parts: (i) interactions that can change the spin and possibly the motional state at the same time (sideband transitions) are associated with the Rabi frequency $\Omega_0$, (ii) interactions that can change only the motional state are associated with the Rabi frequencies $\Omega_s$ with $s\epsilon\{\uparrow,\downarrow\}$, and (iii) pure level shifts $\Delta_s$ due to the ac Stark effect induced independently by each of the two laser beams. Because the energy of the ions internal and/or external degrees of freedom changes in transitions of type (i) and (ii), these interactions can be only resonantly driven by one photon from each of the two electric fields (which also need to have an energy difference appropriate for energy conservation in the process) while the coupling in (iii) is mediated by two photons out of the same electric field (we do not consider the case $\delta_0=0$). The Rabi frequencies are given by sums over dipole matrix elements

$$\Omega_0 = \frac{1}{4\hbar^2}\sum_l \frac{\langle\uparrow|\mathbf{d}\cdot\mathbf{E}_2|l\rangle\langle l|\mathbf{d}\cdot\mathbf{E}_1|\downarrow\rangle}{\Delta_{l1}} + \frac{\langle\uparrow|\mathbf{d}\cdot\mathbf{E}_1|l\rangle\langle l|\mathbf{d}\cdot\mathbf{E}_2|\downarrow\rangle}{\Delta_{l2}},$$

$$\Omega_s = \frac{1}{4\hbar^2}\sum_l \frac{\langle s|\mathbf{d}\cdot\mathbf{E}_2|l\rangle\langle l|\mathbf{d}\cdot\mathbf{E}_1|s\rangle}{\Delta_{l1}} + \frac{\langle s|\mathbf{d}\cdot\mathbf{E}_1|l\rangle\langle l|\mathbf{d}\cdot\mathbf{E}_2|s\rangle}{\Delta_{l2}},$$

$$\Delta_s = \frac{1}{4\hbar^2}\sum_l \frac{|\langle s|\mathbf{d}\cdot\mathbf{E}_1|l\rangle|^2}{\Delta_{l1}} + \frac{|\langle s|\mathbf{d}\cdot\mathbf{E}_2|l\rangle|^2}{\Delta_{l2}}, \tag{2}$$

where $\mathbf{d}$ is the dipole operator (assumed to be real by convention), $\mathbf{E}_1$ and $\mathbf{E}_2$ are the two (real) laser field amplitude vectors, and $\Delta_{lj}=\omega_j-(E_l-E_s)/\hbar$ is the detuning of laser field $j$ ($j\epsilon\{1,2\}$) with respect to the near-resonant level $|l\rangle$. Typically $|\downarrow\rangle$ ($|\uparrow\rangle$) is in the ground-state $S$ manifold with energy $E_\downarrow$ ($E_\uparrow$) while $|l\rangle$ is one of the levels in the first excited $P$ manifold of the ion with energy $E_l$. In the regime of power and detuning of interest for this work [6], the hierarchy $\Delta_l \gg \omega_0 \gg (\Omega_0,\Omega_s,\Delta_s)$ applies. In that case, the choices of $\delta_0$ and $\Delta k$ determine which terms dominate the evolution described by Eq. (1). For $\delta_0\simeq\omega_0$ the terms connected to process (i) are near resonant, leading to spin-flip transitions that can be highly independent of the motion if, in addition, the laser beams are copropagating, leading to $|\Delta\mathbf{k}|\simeq 0$ (see below). For $\delta_0\simeq\omega_m$ and $|\Delta\mathbf{k}|\simeq|\mathbf{k}|$, with $\omega_m$ one of the motional frequencies of the ion(s), process (ii) dominates, leading to state-dependent driving of the motion.

In both situations we would like to suppress (or at least precisely control) the ac Stark shifts (iii) that are inevitable in the presence of the electric fields. In practice we can often balance the ac Stark shifts $\Delta_s$ caused by process (iii) for $|\uparrow\rangle$ and $|\downarrow\rangle$ without diminishing the Rabi frequencies $\Omega_0$ and $\Omega_s$ appreciably by a judicious choice of the intensity and/or polarizations of $\mathbf{E}_1$ and $\mathbf{E}_2$. For example, in $^9Be^+$ two polarizations close to linear and orthogonal to each other can be used to yield $\Delta_\downarrow-\Delta_\uparrow\simeq 0$ and $\Omega_\downarrow\simeq-2\Omega_\uparrow$ for the states $|\uparrow\rangle=|F=1,m_F=-1\rangle$ and $|\downarrow\rangle=|F=2,m_F=-2\rangle$ in the $S_{1/2}$ electronic ground state [20]. On the other hand, we can use only one of the Raman beams (e.g., $\mathbf{E}_1\neq 0$, $\mathbf{E}_2=0$ with $\mathbf{E}_1$ circularly polarized) that induce state-dependent ac Stark shifts to implement rotations around the $z$ axis of the Bloch sphere of the form (up to an irrelevant global phase)

$$Z(\phi)|\uparrow\rangle = e^{i\phi}|\uparrow\rangle,$$

$$Z(\phi)|\downarrow\rangle = e^{-i\phi}|\downarrow\rangle. \tag{3}$$

## IV. PARAXIAL DESCRIPTION OF THE LASER MODES

We assume that all laser beams can be described as having a Gaussian $TEM_{00}$ transverse beam profile. A Gaussian beam with wave vector $k$ and angular frequency $\omega$ propagating along the $z$ axis is the lowest order solution of the paraxial wave equation and can be described by [21]

$$E(\mathbf{r},t) = \frac{E_0}{2}\frac{w_0}{w(z)}\exp\left(\frac{-r^2}{w(z)^2}\right)\exp\left[-i\left(kz-\omega t+\phi - \arctan(z/z_r)+\frac{kr^2}{2R(z)}\right)\right]+\text{c.c.} \quad (4)$$

with $w_0$ the beam waist and

$$w(z) = w_0\sqrt{1+(z/z_r)^2},$$

$$R(z) = z[1+(z_r/z)^2],$$

$$z_r = \frac{kw_0^2}{2}. \quad (5)$$

For simplicity we consider only the situation where $|z| \ll |z_r|$, although it is possible to generalize the formalism to the curved wave fronts in the regions with $|z| \geq |z_r|$. In our region of interest we can write $w(z) \approx w_0$, $\arctan(z/z_r) \approx 0$, and $(kr^2)/[2R(z)] \approx 0$. Under these approximations the beam simplifies to

$$E(\mathbf{r},t) = \frac{E_0}{2}\exp(-r^2/w_0^2)\exp[-i(kz-\omega t+\phi)]+\text{c.c.} \quad (6)$$

This expression describes the salient points of the spatial dependence of the beams in the following discussions.

## V. ONE-QUBIT ROTATIONS

Up to the present, laser-induced one-qubit rotations of trapped ion qubits have been implemented by turning laser beams on and off for a duration appropriate to achieve a certain rotation angle on the Bloch sphere. By also controlling the relative phase of the laser beams, arbitrary rotations on the Bloch sphere can be implemented. Here we propose to move ions precisely through a laser beam to achieve the same level of control. The duration of the interaction is now controlled by the speed $v=|\mathbf{v}|$ of the movement. We assume that the ion under study traverses two copropagating laser beams at an angle $\gamma$ relative to the $k$ vectors [see Fig. 2(a)]. Since the wave vectors of the two laser fields are not exactly equal, their relative phase changes by $\Delta\phi_p \simeq s_0\ \omega_0/c = 2\pi(s_0/\Lambda_0)$ over locations separated by distance $s_0$ along the direction of the beams, where $\Lambda_0$ is the wavelength corresponding to the hyperfine transition frequency of the ion in question. Typically $\omega_0/(2\pi)$ is from 1 GHz to several gigahertz so that in $^9Be^+$, $\omega_0 \simeq 2\pi \times 1.25$ GHz, and $\Lambda_0 \simeq 0.24$ m. Therefore, $\Delta\mathbf{k}\cdot\mathbf{r} = (\mathbf{k}_1 - \mathbf{k}_2)\cdot\mathbf{r}$ can be taken to be constant for the typical variations of $\mathbf{r}$ of a few nanometers, and the effective Hamiltonian equation (1) is highly independent of the ion motion. If the laser frequencies differ by $\delta_0 = \omega_0$, we can drop all rapidly rotating terms in Eq. (1) in a second rotating wave approximation and are left with

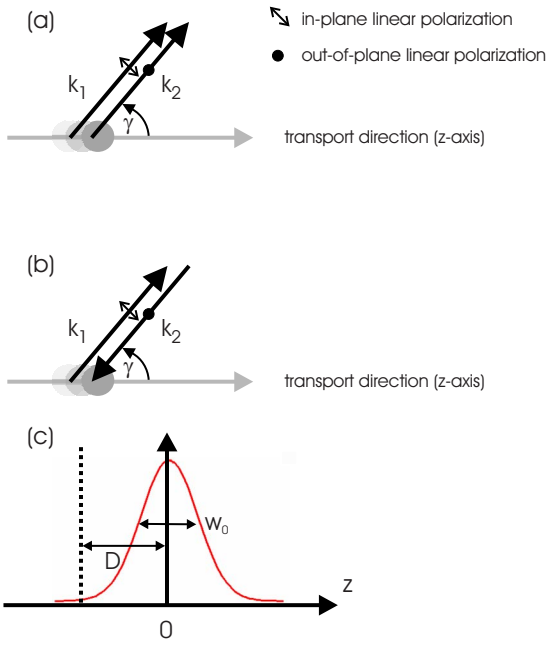


FIG. 2. (Color online) Beam parameters for one- and two-qubit gates: (a) Orientation of the wave vectors $\mathbf{k}_1$ and $\mathbf{k}_2$ relative to the transport direction for copropagating beams as used in the one-qubit rotations. (b) Orientation of the wave vectors $\mathbf{k}_1$ and $\mathbf{k}_2$ relative to the transport direction for counter-propagating beams as used in the two-qubit phase gate. (c) The starting point of the ion trajectory is a distance $D$ from the center of the Gaussian beam profile at $z=0$ with waist size $w_0$.

$$H_{\text{flip}} = \hbar\Omega_0 e^{-i\phi}|\uparrow\rangle\langle\downarrow| + \text{H.c.} \quad (7)$$

leading to Rabi rotations $R(\theta,\phi)$ on the Bloch sphere that can be described by

$$R(\theta,\phi)|\uparrow\rangle = \cos(\theta/2)|\uparrow\rangle - ie^{i\phi}\sin(\theta/2)|\downarrow\rangle,$$

$$R(\theta,\phi)|\downarrow\rangle = -ie^{-i\phi}\sin(\theta/2)|\uparrow\rangle + \cos(\theta/2)|\downarrow\rangle. \quad (8)$$

For simplicity we assume that both beams have the same transverse mode function as given by Eq. (6). The trajectory is such that the ion is located in the center of the beams at $t=0$, where it experiences the maximum coupling strength $\Omega_m$, which can be calculated by inserting $E_0$ of Eq. (6) into $\Omega_0$ of Eq. (2). The time-dependent Raman-coupling strength is then

$$\Omega(t) = \Omega_m \exp\{-2[v\sin(\gamma)t/w_0]^2\}. \quad (9)$$

Integration of Eq. (9) gives the rotation angle $\theta$ on the Bloch sphere resulting from a single traverse of the beams starting at time $-T$ and ending at $T$,

$$\theta = \int_{-T}^{T} \Omega(t)dt = \Omega_m \frac{w_0}{v \sin(\gamma)} \sqrt{\frac{\pi}{2}} \mathrm{erf}[\sqrt{2} v \sin(\gamma) T/w_0], \tag{10}$$

where $\mathrm{erf}(z) = (2/\sqrt{\pi}) \int_0^z e^{-t^2} dt$ is the error function. In practice, it is permissible to neglect effects due to the finite distance of the transport start and end points from the center of the modes ($T \to \infty$), in which case $\mathrm{erf}[\sqrt{2} v \sin(\gamma) T/w_0] \to 1$ in Eq. (10). The relative error $\Delta\theta/\theta$ introduced by this approximation is $\Delta\theta/\theta = 1 - \mathrm{erf}[\sqrt{2} D \sin(\gamma)/w_0]$, where $D$ is the initial distance of the ion from the center of the beams [see Fig. 2(c)]. As an example, if $\gamma = \pi$ (beams perpendicular to the trajectory), the infidelity $1 - F \simeq (\Delta\theta/\theta)^2$ is smaller than $10^{-4}$ if $D > 2.6\ w_0$. Based on this path length of $2.6\ w_0$ we can compare the approximate duration $T_t$ to execute a transport gate with angle $\theta$ to the duration $T_s$ necessary for the same rotation if the ion resides in the center of beams that are switched on and off suddenly, yielding $T_t/T_s = 2.6\sqrt{2/\pi} \simeq 2.07$.

The exact value of $\theta$ can be controlled by the speed with which the ion is transported through the beams. For example, to execute a $\pi$ pulse given a waist size of $w_0 = 20\ \mu$m and $\Omega_m = 250$ kHz, we need a velocity $v \simeq 25$ m/s. Similar transport speeds (average speed 25 m/s and a peak velocity of about 45 m/s), while keeping a single ion in the ground state of the transported potential well, have been demonstrated previously [4]. Moreover, the ground state does not need to be preserved for single-qubit rotations (using copropagating beams), so faster, nonadiabatic transport is possible if the ion can be sympathetically recooled after a rotation [2,3].

The angle $\phi$ on the Bloch sphere is controlled by the relative phase of the laser fields at $\mathbf{r}_{\mathrm{lab}}$. This phase changes by $\Delta\phi_p \simeq 2\pi(s_0/\Lambda_0)$ between two interaction zones utilizing the same beams that are separated by a beam path of length $s_0$. Independent of whether or not temporal laser pulses or transport gates are used, $\Delta\phi_p$ cannot be neglected over an extended trap array. It is necessary to do careful bookkeeping of phases over an extended trap array to properly set and control operations. If the same pair of beams is used for one-qubit rotations in several different places, we do not have the freedom of setting $\phi$ independently for all these rotations. There are several ways to deal with this problem. For example, a straightforward, but logistically costly, solution would be to transport a given ion to a location where $\phi$ happens to be correct for the rotation scheduled on that ion. A more flexible strategy would be to have a discrete set of different relative phases that could be implemented by several beam pairs that are turned on in parallel to address separate locations or by sequentially switching the relative phase of the same beam (universal computation can be achieved with a discrete set of one-qubit rotations [22]). The time overhead caused by such sequential rotations may not slow down the computation considerably, because one-qubit rotations are typically much faster than two-qubit gates.

We could also momentarily turn on only one of the Raman beams. Transporting the ion through that beam with a certain velocity induces time-dependent ac Stark shifts that can be used to achieve rotations $Z(\phi)$ [see the discussion preceding Eq. (3)]. A given rotation $R(\theta_2, \phi)$ with $\phi$ fixed can be turned into an arbitrary one-qubit rotation $U$ by sandwiching it between two $Z$ operations, $U = e^{i\phi_4} Z(\phi_3) R(\theta_2, \phi) Z(\phi_1)$ [22]. In the context of a multioperation algorithm, this can be further simplified: The final operation $Z(\phi_3)$ does not affect measurement outcomes and can therefore be neglected in a one-qubit operation that precedes a measurement. This also holds if two-qubit phase gates are applied before the measurement since all $Z(\phi)$ commute with phase gates [23]. For all other operations the final step of the previous rotation $Z_{\mathrm{prev}}(\phi_3)$ can be combined into the next one-qubit manipulation $U' = R(\theta_2', \phi') Z'(\phi_1')$ where $Z'(\phi_1') = Z(\phi_1') Z_{\mathrm{prev}}(\phi_3) = Z(\phi_1' + \phi_3)$. Thus, transporting the qubit ion through one laser beam first and then through two beams with detuning $\omega_0$ at the appropriate velocity is sufficient for implementing universal one-qubit manipulations.

## VI. TWO-QUBIT GATES

For the two-qubit gate we consider two ions trapped in the same harmonic well. If the frequency difference of the two Raman beams is close to a motional frequency $\omega_m$ and much smaller than the qubit level frequency difference, $\delta_0 \ll \omega_0$, we can neglect terms rotating with $\omega_0$ in Eq. (1). Then the effective Hamiltonian of the ions can be approximated by

$$\begin{aligned} H_{zz} = \hbar[\Omega_\uparrow(\mathbf{r}_1)|\uparrow 1\rangle\langle\uparrow 1| + \Omega_\downarrow(\mathbf{r}_1)|\downarrow 1\rangle\langle\downarrow 1|] e^{-i(\delta_0 t + \phi)} e^{i\Delta\mathbf{k}\cdot\mathbf{r}_1} \\ + \mathrm{H.c.} + \hbar[\Omega_\uparrow(\mathbf{r}_2)|\uparrow 2\rangle\langle\uparrow 2| + \Omega_\downarrow(\mathbf{r}_2)|\downarrow 2\rangle \\ \times\langle\downarrow 2|] e^{-i(\delta_0 t + \phi)} e^{i\Delta\mathbf{k}\cdot\mathbf{r}_2} + \mathrm{H.c.}, \end{aligned} \tag{11}$$

where $\mathbf{r}_1$ and $\mathbf{r}_2$ are the positions of the two ions. We use a shorthand notation for the two-qubit operators $|\uparrow 1\rangle\langle\uparrow 1| \otimes = |I2\rangle\langle I2| \equiv |\uparrow 1\rangle\langle\uparrow 1|$ and so on, suppressing identity operators $I$. Two ions in the same harmonic potential well perform normal-mode oscillations around their equilibrium position. We choose coordinates such that the axis along which the ion conformation aligns coincides with the transport direction ($z$ axis). The equilibrium distance is determined by the balance of Coulomb repulsion and the restoring forces of the external potential and is given by $d = [q^2/(2\pi\epsilon_0 m \omega_{\mathrm{COM}}^2)]^{1/3}$, with $\epsilon_0$ the vacuum permittivity, $m$ the mass, and $\omega_{\mathrm{COM}}$ the center-of-mass oscillation frequency of the ions [2]. We can rewrite the ion positions as $\mathbf{r}_1 = \mathbf{r}_0 + d/2\ \mathbf{e}_z + \delta\mathbf{r}_1$ and $\mathbf{r}_2 = \mathbf{r}_0 - d/2\ \mathbf{e}_z + \delta\mathbf{r}_2$, where $\mathbf{r}_0$ coincides with the minimum of the harmonic potential, $\mathbf{e}_z$ is a unit vector along the $z$ axis and $\delta\mathbf{r}_j$ describes the small displacements of ion $j$ around it's equilibrium position. Substituting $\mathbf{r}_0 \to \mathbf{r}_{\mathrm{lab}} + \mathbf{v}\ t$, we can neglect the overall phase factor $\phi + \Delta\mathbf{k}\cdot\mathbf{r}_{\mathrm{lab}}$ that is common to both ions and, as long as it is constant over the time of a gate interaction, does not change the logical phase of the gate. Therefore, in contrast to the one-qubit rotations, no bookkeeping of $\phi$ over the trap array is necessary. We include the Doppler shift $\Delta\mathbf{k}\cdot\mathbf{v}t$ in $\delta_0$, define $\varphi \equiv \Delta k_z d/2$, and make the Lamb-Dicke approximation, so that $\exp(i\Delta\mathbf{k}\cdot\delta\mathbf{r}_j) \simeq 1 + i\Delta\mathbf{k}\cdot\delta\mathbf{r}_j$, which is valid whenever the excursions $|\delta\mathbf{r}_j|$ are small enough that $|\Delta\mathbf{k}\cdot\delta\mathbf{r}_j| \ll 1$. We also neglect the small differences in Rabi

frequency due to the different positions of the two ions within the Gaussian beam (assuming $d \ll w_0$) and set $\Omega_s(\mathbf{r}_j) \simeq \Omega_s(\mathbf{r}_0)$ $(s \epsilon \{\uparrow, \downarrow\})$.

Using these definitions and approximations we can rewrite Eq. (11):

$$H_{zz} \simeq \hbar[\Omega_\uparrow(\mathbf{r}_0)|\uparrow 1\rangle\langle\uparrow 1| + \Omega_\downarrow(\mathbf{r}_0)|\downarrow 1\rangle\langle\downarrow 1|]e^{-i(\delta_0 t+\varphi)} \times(1 + i\Delta\mathbf{k}\cdot\delta\mathbf{r}_1) + \text{c.c.} + \hbar[\Omega_\uparrow(\mathbf{r}_0)|\uparrow 2\rangle\langle\uparrow 2| + \Omega_\downarrow(\mathbf{r}_0)|\downarrow 2\rangle\langle\downarrow 2|]e^{-i(\delta_0 t-\varphi)}(1 + i\Delta\mathbf{k}\cdot\delta\mathbf{r}_2) + \text{c.c.} \tag{12}$$

We can now replace the small displacements $\delta\mathbf{r}_j$ by the corresponding sum of all normal-mode displacements, including those in the directions orthogonal to $\mathbf{e}_z$. For two ions of equal mass the two normal modes along the $z$ axis are an in-phase [center-of-mass, (COM)] oscillation of both ions at frequency $\omega_{\text{COM}}$ and out-of-phase [stretch, (str)] oscillation at frequency $\omega_{\text{str}} = \sqrt{3}\omega_{\text{COM}}$ with normal coordinates $z_{\text{COM}} = 1/\sqrt{2}(\delta\mathbf{r}_1 + \delta\mathbf{r}_2)\cdot\mathbf{e}_z$ and $z_{\text{str}} = 1/\sqrt{2}(\delta\mathbf{r}_1 - \delta\mathbf{r}_2)\cdot\mathbf{e}_z$. To be specific, we concentrate on detuning $\delta_0 \simeq \omega_{\text{str}}$ close to the stretch mode frequency, so that $|\delta_0 - \omega_{\text{str}}| \ll \{\omega_{\text{COM}}, \omega_{\text{str}}, \omega_{\text{str}} - \omega_{\text{COM}}\}$. In the interaction picture, each normal-mode position operator has the same form as the stretch mode operator,

$$z_{\text{str}} = \sqrt{\frac{\hbar}{2m\omega_{\text{str}}}}(ae^{-i\omega_{\text{str}}t} + a^\dagger e^{i\omega_{\text{str}}t}), \tag{13}$$

with $\omega_{\text{str}}$ replaced by the corresponding mode frequency. Here $a^\dagger(a)$ is the harmonic oscillator mode creation (destruction) operator. Once inserted into Eq. (12), all rapidly oscillating terms average to zero and are neglected in the following: we keep the near-resonant term, which is proportional to $e^{\pm i(\delta_0 - \omega_{\text{str}})}$. Substituting the normal coordinates, setting $\eta = \Delta\mathbf{k}\cdot\mathbf{e}_z\sqrt{\hbar/(2m\omega_{\text{str}})}$, and making the definition $\delta \equiv \omega_{\text{str}} - \delta_0$, we obtain

$$H_{zz} \simeq i\hbar\eta\sum_{s,s'}(A_{ss'}e^{i\delta t}a^\dagger - A^*_{ss'}e^{-i\delta t}a)|ss'\rangle\langle ss'|, \tag{14}$$

with $s$, $s' \epsilon \{\uparrow, \downarrow\}$, $|ss'\rangle\langle ss'| \equiv |s1\rangle\langle s1| \otimes |s'2\rangle\langle s'2|$, and

$$A_{\uparrow\uparrow} = -\sqrt{2}i\sin(\varphi)\Omega_\uparrow,$$

$$A_{\uparrow\downarrow} = \frac{1}{\sqrt{2}}(\Omega_\uparrow e^{-i\varphi} - \Omega_\downarrow e^{i\varphi}),$$

$$A_{\downarrow\uparrow} = \frac{1}{\sqrt{2}}(\Omega_\downarrow e^{-i\varphi} - \Omega_\uparrow e^{i\varphi}),$$

$$A_{\downarrow\downarrow} = -\sqrt{2}i\sin(\varphi)\Omega_\downarrow. \tag{15}$$

The Hamiltonian $H_{zz}$ generates a time-dependent and internal-state-dependent coherent drive [24] resulting from state-dependent dipole forces on the ions. Since the infinitesimal generator of the evolution $H_{zz}$ does not commute with itself for different times, and $\delta \neq 0$, the evolution needs to be calculated with either a time-ordered integral approach [25] or another method that properly evaluates the acquired state-dependent phase. As briefly described in the methods section of Ref. [26], we can start from the infinitesimal displacement $d\alpha(t) = \eta A_{ss'}e^{i\delta t}$ generated by $H_{zz}$ and calculate the total coherent displacement

$$\alpha(t) = \int_{t_0}^{t} d\alpha(t')dt' = \eta A_{ss'}\int_{t_0}^{t} e^{i\delta t'}dt', \tag{16}$$

and the acquired phase

$$\Phi(t) = \text{Im}\left(\int_{t_0}^{t}\alpha^*(t')d\alpha(t')dt'\right) = \text{Im}\left[\int_{t_0}^{t}\left(\int_{t_0}^{t'}d\alpha^*(t'')dt''\right)d\alpha(t')dt'\right], \tag{17}$$

to express the evolution $U_{zz}(t) = \exp(i\Phi)\exp\{i[\alpha(t)a^\dagger - \alpha^*(t)a]\}$ caused by $H_{zz}$. We can now restrict our attention to the special case of two Gaussian beams of equal frequency that have approximately orthogonal polarization and counterpropagate with $\mathbf{k}_1 = -\mathbf{k}_2 = \mathbf{k}$ [a polarization gradient standing wave, see Fig. 2(b)], with angles $\gamma$ and $\pi + \gamma$, respectively, to the transport direction of the ion pair. In the frame of reference of the moving ions, the beams are Doppler shifted by $\Delta\omega = \pm|k||v|\cos(\gamma)$, respectively, setting the relative detuning of the beams to

$$\delta_0 = 2|k||v|\cos(\gamma). \tag{18}$$

As in the discussion before Eq. (9) we assume that both beams have the same transverse mode function given by Eq. (6), and the trajectory is such that the ions traverse the center of the beams at $t=0$, where they experience the maximum coupling strength $\Omega_{s,m}$ with $s \epsilon \{\uparrow, \downarrow\}$. The time-dependent Raman-coupling strength is then

$$\Omega_s = \Omega_{s,m}\exp\{-2[v\sin(\gamma)t/w_0]^2\}. \tag{19}$$

We can define the approximate transit duration of the ions through the beam $\tau \equiv w_0/[\sqrt{2}v\sin(\gamma)]$. Since the Gaussian envelope is common to both $\Omega_s$, we can rewrite Eq. (15) as

$$A_{s,s'}(t) = A^0_{s,s'}e^{-t^2/\tau^2}, \tag{20}$$

with $A^0_{s,s'} \equiv A_{s,s'}(t=0)$. It is then straightforward to solve the integral for the mode displacement in phase space (16),

$$\alpha_{ss'}(t) = \eta A^0_{ss'}\int_{-t}^{t} e^{-t'^2/\tau^2 + i\delta t'}dt' = e^{-\delta^2\tau^2/4}\frac{\sqrt{\pi}\eta A^0_{ss'}\tau}{2}\left[\text{erf}\left(t/\tau - \frac{i\delta\tau}{2}\right) + \text{erf}\left(t/\tau + \frac{i\delta\tau}{2}\right)\right]. \tag{21}$$

For the final displacement, after the ions have traversed a distance equal to several beam waists, we can evaluate Eq. (20) at $t=\infty$ and find

$$\alpha_{ss'}(\infty) = e^{-\delta^2\tau^2/4}\sqrt{\pi}\eta A^0_{ss'}\tau. \tag{22}$$

This expression shows that the end point of the trajectory can be $\alpha_{ss'}(\infty) \neq 0$. However, by choosing $\delta\tau/\sqrt{2}$ large we can bring the end point exponentially close to zero. This is im-

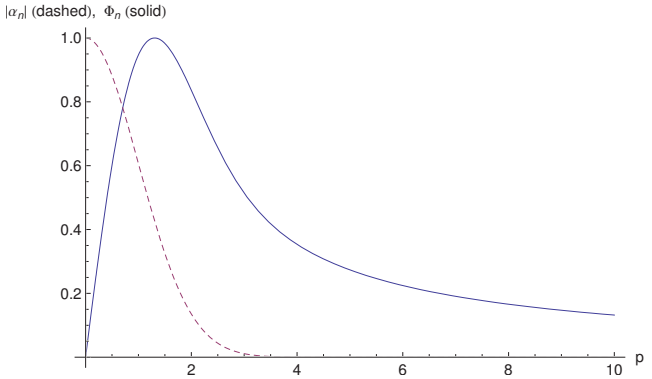


FIG. 3. (Color online) Normalized modulus of the final coherent state amplitude $\alpha_n=|\alpha_{ss'}(\infty)|/|\alpha_{ss'}(0)|$ (dashed line) and normalized phase $\Phi_n=\Phi_{ss'}/\max(\Phi_{ss'})$ (solid line) as a function of $p$.

portant since we need the motional state of the ions to be disentangled from the internal states after the gate is executed. The simplest way to achieve this is to make sure that the final displacement for all combinations of internal states is zero, or very close to zero. We return to this point and its implications for the gate fidelity below.

It is also worth noting that from Eq. (21), $\alpha_{ss'}(\infty)$ is proportional to the Fourier transform of the pulse envelope at frequency $\delta$. This implies that we can make the final displacements very small for any choice of envelope that has small Fourier components at $\delta$, and the transport gates also work for beam shapes that deviate from Gaussian as long as they are reasonably smooth.

For the logic phases after a complete transit through the beam we need to solve the integral

$$\Phi_{ss'} = |\eta A^0_{ss'}|^2 \,\mathrm{Im}\left[\int_{-\infty}^{\infty}\left(\int_{-\infty}^{t'} e^{-t''^2/\tau^2 - i\delta t''}dt''\right)e^{-t'^2/\tau^2 + i\delta t'}dt'\right]$$
$$= |\eta A^0_{ss'}|^2 \,\mathrm{Im}\left(\int_{-\infty}^{\infty}\int_{-\infty}^{t'} e^{-t''^2/\tau^2 - i\delta t'' - t'^2/\tau^2 + i\delta t'}dt''dt'\right). \tag{23}$$

A coordinate transformation $t''=(u-v)/\sqrt{2}$, $t'=(u+v)/\sqrt{2}$ lifts the interdependence of the integrals, leading to a closed form solution

$$\Phi_{ss'} = |\eta A^0_{ss'}|^2 \,\mathrm{Im}\left(\int_{-\infty}^{\infty} e^{-u^2/\tau^2}du\int_{0}^{\infty} e^{-v^2/\tau^2 + i\sqrt{2}\delta v}dv\right)$$
$$= |\eta A^0_{ss'}|^2 \tau^2 \frac{e^{-\delta^2\tau^2/2}\pi\,\mathrm{erfi}\left(\frac{\delta\tau}{\sqrt{2}}\right)}{2}, \tag{24}$$

where $\mathrm{erfi}(z)=-i\,\mathrm{erf}(iz)$. Figure 3 shows $\alpha_{ss'}(\infty)$ and $\Phi_{ss'}$, both normalized to their respective maximal values as a function of the parameter $p\equiv\delta\tau/\sqrt{2}$. It gives insight into the trade off necessary to meet the requirement $|\alpha_{ss'}(\infty)|\simeq 0$. While $\alpha_{ss'}(\infty)$ decays exponentially in $p^2$, $\Phi_{s,s'}$ decays more slowly with $p$ due to its dependence on the complex error function, so that even for very small values of $|\alpha_{ss'}(\infty)|$ the value of $\Phi_{ss'}$ remains at an appreciable fraction of its maximal value. Note that we could also use two well-aligned transits through two beam pairs (or the same beam pair). The acquired gate phase would add for the two passes, while the displacements can be arranged to be opposite, so the motional state returns to the origin. However, for this approach to be viable the timing would have to be controlled to a small fraction of $2\pi/\delta$, which seems imposing, while a sufficiently small $|\alpha_{ss'}(\infty)|$ turns out to be easily achieved for reasonably large $p$ (see below). The resulting phase gate differs by only one-qubit $z$ rotations from the standard phase gate,

$$U(\Phi_L) = |\uparrow\uparrow\rangle\langle\uparrow\uparrow| + |\uparrow\downarrow\rangle\langle\uparrow\downarrow| + |\downarrow\uparrow\rangle\langle\downarrow\uparrow| + e^{i\Phi_L}|\downarrow\downarrow\rangle\langle\downarrow\downarrow|, \tag{25}$$

and the total logical phase of the gate can be written as $\Phi_L=\Phi_{\uparrow\uparrow}+\Phi_{\downarrow\downarrow}-(\Phi_{\uparrow\downarrow}+\Phi_{\downarrow\uparrow})$ [27]. We find

$$\Phi_L = -\pi e^{-\delta^2\tau^2/2}\,\mathrm{erfi}\left(\frac{\delta\tau}{\sqrt{2}}\right)\frac{1}{2}\eta^2(\Omega_\uparrow-\Omega_\downarrow)^2\tau^2\cos(2\varphi). \tag{26}$$

This expression shows that the largest modulus of the logical phase is achieved for $\cos(2\varphi)=\pm 1$, corresponding to $\Delta k_z d=n\pi$ with $n$ integer. Therefore, the ion spacing should be a multiple of the one-half period of the polarization gradient wave along the transport direction $z$. From now on we assume the ion distance is adjusted (by a proper choice of the curvature of the transported harmonic well) to yield a maximum modulus for the logical phase [26,28]. This implies that $A^0_{\uparrow\uparrow}=A^0_{\downarrow\downarrow}=0$ and $|A^0_{\uparrow\downarrow}|^2=|A^0_{\downarrow\uparrow}|^2=1/2(\Omega_\uparrow-\Omega_\downarrow)^2$. For a gate equivalent to a $\pi$-phase gate we then require $\Phi_L=-\pi$, equivalent to

$$e^{-\delta^2\tau^2/2}\frac{1}{2}\eta^2(\Omega_\uparrow-\Omega_\downarrow)^2\tau^2\,\mathrm{erfi}\left(\frac{\delta\tau}{\sqrt{2}}\right)=1. \tag{27}$$

With this condition, and assuming that the trajectory of the ions starts at $\alpha_{\uparrow\downarrow}(t=-\infty)=0$, we can derive an expression for the phase space trajectory $\alpha_{\uparrow\downarrow}(t)$ that depends only on $p$ [29],

$$\alpha_{\uparrow\downarrow}(t) = \frac{\sqrt{\pi}\left[\mathrm{erf}\left(t/\tau-\frac{ip}{\sqrt{2}}\right)+1\right]}{2\sqrt{\mathrm{erfi}(p)}}. \tag{28}$$

If we assume that the only source of error in the gate is the incomplete return to the origin for states that acquire a phase, the fidelity of a gate can be bounded from below by the worst-case overlap of the final state with the trap ground state,

$$F \geq \min_{\{c_{ss'}\}}\left|\sum_{s,s'} c_{ss'}\langle\alpha_{ss'}(\infty)|0\rangle\right|^2 = \min_{\{c_{ss'}\}}\left|\sum_{s,s'} c_{s,s'}e^{-|\alpha_{ss'}(\infty)|^2/2}\right|^2$$
$$= e^{-|\alpha_{\uparrow\downarrow}(\infty)|^2} \simeq 1-|\alpha_{\uparrow\downarrow}(\infty)|^2, \tag{29}$$

where $c_{ss'}$ are the amplitudes for state $|ss'\rangle$ in an arbitrary two-qubit spin state the gate is operating on. Using Eq. (27) and Eq. (21) we find

$$\epsilon = 1-F \leq \pi/\mathrm{erfi}(p). \tag{30}$$

We assume that subsequent gates are implemented after sympathetic recooling to the motional ground state, preventing coherent addition of errors of this type.

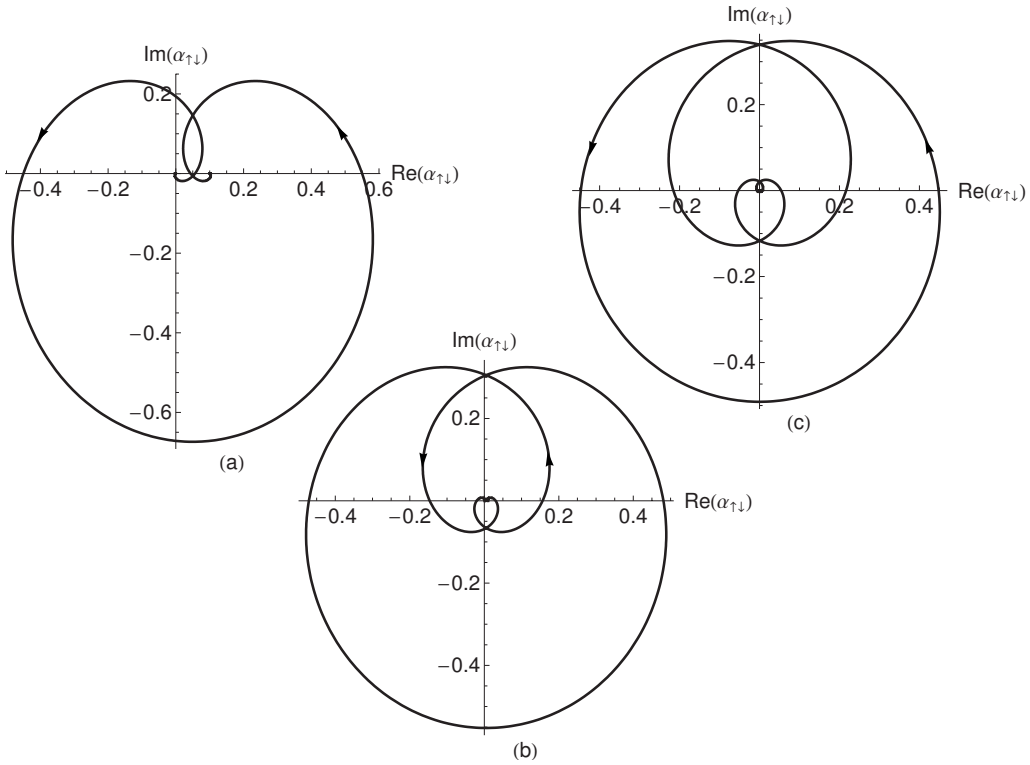


FIG. 4. Phase space trajectories of the state $|\uparrow\downarrow\rangle$ for (a) $\epsilon \leq 10^{-2}$ ($p=2.69$), (b) $\epsilon \leq 10^{-4}$ ($p=3.48$), and (c) $\epsilon \leq 10^{-6}$ ($p=4.11$). The arrows indicate the trajectory directions. The trajectories are fully determined (up to their orientation in phase space) by $p$ and the requirement that the logical phase is $\Phi_L=-\pi$.

The trajectories in phase space of the $|\uparrow\downarrow\rangle$ state, as described by Eq. (28) for phase gates with $\epsilon \leq 10^{-2}$ ($p=2.69$), $\epsilon \leq 10^{-4}$ ($p=3.48$), and $\epsilon \leq 10^{-6}$ ($p=4.11$), are shown in Fig. 4. For large $|t|$, the trajectory spirals near the origin and the number of windings per time interval $\tau$ increases as $p$ is increased. Any desired proximity to the origin can be realized by making $p$ large enough. We can therefore also think of $p$ as a gate-adiabatic parameter, because no motional energy is deposited in the system for $p \to \infty$.

In practice it is interesting to note that $\delta_0 \tau/\sqrt{2} = k w_0 \cot(\gamma)$ is independent of the transport speed and is basically a measure of how many periods of the polarization gradient wave are encountered by the ions while they are traveling through the central portion of the beam. Unless the beam is very strongly focused, we have $kw_0 \gg 1$, and the ions sample many periods of the polarization gradient wave. By choosing $\gamma$ close to 90° We can reduce the number of periods encountered, but there are drawbacks to such a choice. On the one hand, $\eta \propto \cos(\gamma)$ becomes small. As can be seen from Eq. (27) a smaller $\eta$ must be compensated for somehow, for example, by a higher Rabi rate that requires more laser power could lead to excitation of off-resonant terms in Eq. (12) and cause increased decoherence from spontaneous emission [6]. In addition, to fulfill the requirement $\cos(2\phi) = \pm 1$, we must restrict the angle $\gamma$ to discrete values given by

$$\Delta k_z d = 2k \cos(\gamma_n)[q^2/(2\pi\epsilon_0 m \omega_{\mathrm{COM}}^2)]^{1/3} = n\pi, \qquad (31)$$

with $\gamma$ closest to $\pi$ for $n=1$. We can still choose different values for $\gamma$ by not requiring $\cos(2\phi)=\pm 1$, but at the price of achieving a less than optimal logical phase.

To assess the practical feasibility of such a gate, we assume parameters for two $^9Be^+$ ion qubits that are achieved in current experiments at NIST, namely an axial trap frequency of $\omega_{\mathrm{COM}}=2\pi\times 4$ MHz, a beam waist of $w_0=20$ $\mu$m, $\Omega_\uparrow = -1/2\Omega_\downarrow$, and a wavelength of 313 nm. We further impose $p=3.48$ to ensure that $\epsilon \leq 10^{-4}$. For $n<10$ the necessary detuning $\delta$ ranges from 29.63 MHz to 768 kHz, too large to reasonably fulfill $|\delta| \gg \omega_{\mathrm{COM}}$; therefore, only a more complete theory that takes the faster rotating terms into account in Eq. (12) would yield meaningful results. As Table I shows, the transport speed $v_n$ is reasonable for all $n \geq 10$, and gates with duration $\tau_n$ on the order of 1 $\mu$s can be realized if enough laser power is available to produce the Rabi frequencies $\Omega_\downarrow$. Gate times are around 5 $\mu$s, comparable to the present state of the art with phase gates, require $\gamma$ to be between 60° and 40° and Rabi frequencies that are close to values that have been realized in previous experiments at NIST.

## VII. EFFECTS OF SYMPATHETIC COOLING

An integral part of QIP with ions in a large trap array is sympathetic cooling of the qubit ions with "refrigerator" ions [2,3,30–32] to remove excess motional energy after transport and to reset the motional modes into a well-defined initial quantum state. Sympathetic cooling requires the presence of neighboring ions during gate operations; these were not considered in the preceding sections. Although the presence of extra ions complicates the description of two qubit gates, it does not change the essential features of the method. There

TABLE I. Gate parameters for an axial trap frequency of $\omega_{\mathrm{COM}}=2\pi\times 4$ MHz, beam waist of $w_0=20$ $\mu$m, $\Omega_{\uparrow}=-1/2$ $\Omega_{\downarrow}$, wavelength of 313 nm ($^9Be^+$) and $p=3.48$ ($\epsilon\leq 10^{-4}$). All parameters, including Rabi frequencies $\Omega_{\downarrow}$, are within experimental reach.

| $n$ | $\gamma$/deg | $\eta$ | $\upsilon$/(m/s) | $\tau/\mu$s | $\delta/(2\pi$ MHz) | $\Omega_{\downarrow}/(2\pi$ MHz) |
|---|---|---|---|---|---|---|
| 10 | 77.6 | 0.077 | 5.50 | 1.32 | 0.596 | 3.579 |
| 12 | 75.1 | 0.093 | 4.52 | 1.62 | 0.484 | 2.423 |
| 14 | 72.6 | 0.108 | 3.83 | 1.93 | 0.405 | 1.738 |
| 16 | 70.0 | 0.124 | 3.32 | 2.26 | 0.346 | 1.300 |
| 18 | 67.3 | 0.139 | 2.94 | 2.61 | 0.300 | 1.003 |
| 20 | 64.7 | 0.155 | 2.63 | 2.98 | 0.263 | 0.791 |
| 22 | 61.9 | 0.170 | 2.38 | 3.37 | 0.233 | 0.636 |
| 24 | 59.1 | 0.186 | 2.17 | 3.79 | 0.207 | 0.518 |
| 26 | 56.2 | 0.201 | 2.00 | 4.25 | 0.184 | 0.426 |
| 28 | 53.2 | 0.217 | 1.85 | 4.77 | 0.164 | 0.353 |
| 30 | 50.1 | 0.232 | 1.72 | 5.35 | 0.147 | 0.293 |
| 32 | 46.8 | 0.247 | 1.61 | 6.02 | 0.130 | 0.245 |
| 34 | 43.3 | 0.263 | 1.51 | 6.80 | 0.115 | 0.204 |
| 36 | 39.6 | 0.278 | 1.43 | 7.77 | 0.101 | 0.168 |
| 38 | 35.6 | 0.294 | 1.35 | 9.00 | 0.087 | 0.138 |
| 40 | 31.1 | 0.309 | 1.28 | 10.69 | 0.073 | 0.110 |
| 42 | 26.0 | 0.325 | 1.22 | 13.26 | 0.059 | 0.085 |
| 44 | 19.7 | 0.340 | 1.16 | 18.13 | 0.043 | 0.059 |
| 46 | 10.1 | 0.356 | 1.10 | 36.41 | 0.022 | 0.028 |

are more normal modes of motion in the extended ion configuration and it is more complex to properly describe the individual motional amplitudes, especially in a configuration with ions having considerably different masses. Despite these complications the basic gate mechanism is almost unchanged. We consider an ion configuration with a motional eigenmode with frequency $\omega_v$ and normalized eigenvector $\mathbf{v}$. We denote the components (amplitudes) of $\mathbf{v}$ corresponding to the ion qubits as $v_1$ and $v_2$ (both are real numbers) and substitute these into Eq. (12). In complete analogy to the calculation following that equation, we arrive at the generalized displacement coefficients

$$A_{\uparrow\uparrow} = (v_1 e^{-i\varphi} + v_2 e^{i\varphi})\Omega_{\uparrow},$$

$$A_{\uparrow\downarrow} = v_1 e^{-i\varphi}\Omega_{\uparrow} + v_2 e^{i\varphi}\Omega_{\downarrow},$$

$$A_{\downarrow\uparrow} = v_1 e^{-i\varphi}\Omega_{\downarrow} + v_2 e^{i\varphi}\Omega_{\uparrow},$$

$$A_{\downarrow\downarrow} = (v_1 e^{-i\varphi} + v_2 e^{i\varphi})\Omega_{\downarrow}. \tag{32}$$

Calculating the logical phase we obtain the analog to Eq. (26),

$$\Phi_L = \pi e^{-\delta^2\tau^2/2}\,\mathrm{erfi}\left(\frac{\delta\tau}{\sqrt{2}}\right) 2v_1 v_2 \eta^2 (\Omega_{\uparrow} - \Omega_{\downarrow})^2 \tau^2 \cos(2\varphi). \tag{33}$$

Again the logical phase is optimal if the spacing of the qubit ions $d_{12}$ is such that $\Delta k_z d_{12} = n\pi$ with $n$ integer. The suitability of a certain mode for a phase gate can be judged by the factor $v_1 v_2\ \eta^2$. Both amplitudes should be as large as possible, while $\eta^2 \propto 1/\omega_v$ should be not too small. At the same time, the refrigerator ions should not have components in $v$ that are too small, so that sympathetic cooling is efficient. These requirements are probably best satisfied with two ion species of comparable mass in a configuration with reflection symmetry in the $z$ direction [for example, $(q,r,r,q)$ or $(r,q,q,r)$, where $q$ denotes a qubit and $r$ a refrigerator ion].

The normal modes are then still eigenstates of the reflection operation around $z=0$, and therefore $v_1=\pm v_2$. For "stretch-type" modes with $v_1=-v_2$, the optimal coefficients fulfill $A^0_{\uparrow\uparrow}=A^0_{\downarrow\downarrow}=0$ and $|A^0_{\uparrow\downarrow}|^2=|A^0_{\downarrow\uparrow}|^2=v_1^2(\Omega_{\uparrow}-\Omega_{\downarrow})^2$; furthermore, these modes should be better protected from heating because they couple only to field fluctuations that have an appreciable gradient over the ion configuration [33].

One interesting aspect of sympathetic cooling in the strongly adiabatic regime ($p \gg 1$) was already pointed out by Sørensen and Mølmer [34]. Due to the small deviation of the motional wave packets from the origin and the quick succession of revolutions in phase space, the gate becomes more robust to photon recoil and heating of the motion (see also [6]). Therefore, such gates can be executed with reasonable fidelity as long as the heating rate (in quanta per second) is small compared to the rate of revolution in phase space that is set by $\delta$, more precisely, $(dn/dt)T_r \ll 1$, where $T_r$ is the time to complete one revolution in phase space. Gates can even be executed while the ions are recooled sympathetically, as long as the combined rates of phonon scattering due to heating and cooling are small compared to $\delta$. This could be advantageous when very small trap structures are used and the ions are in close proximity to electrode surfaces,

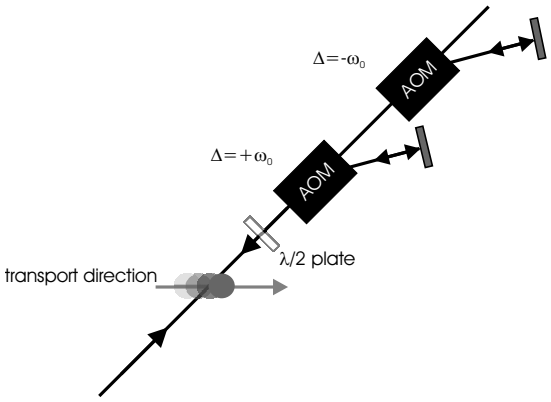


FIG. 5. Possible configuration for the transport version of a Sørensen and Mølmer gate. The two double-pass acousto-optic modulators (AOMs) shift the retroreflected beams by $\pm\omega_0$, respectively. Together with the Doppler shift due to the transport, the ion experiences beat notes close to its blue and red sidebands on the stretch mode that implement the gate.

since the heating rate has been observed to scale strongly with the distance to the nearest surface [35–38]. Sympathetic cooling can ensure that the motional state stays in the Lamb-Dicke regime, even if the unchecked heating rate would drive the ions out of this regime during a gate operation.

## VIII. EXTENSIONS

Hyperfine ground states with an energy splitting that is first-order insensitive to fluctuations in the magnetic field have nearly identical ac Stark shifts, leading to $\Omega_\uparrow \simeq \Omega_\downarrow$ [39–41]. As can be seen from Eq. (26) only a negligible logical phase can be acquired in this situation. This problem can be solved in different ways. If single-qubit rotations of high fidelity are available, one can transfer out of the field-independent manifold into states with $\Omega_\uparrow \neq \Omega_\downarrow$ for the duration of the two-qubit gate operation, followed by transferring back. The ambient magnetic field fluctuations typically do not vary appreciably over the gate time; therefore phase errors can be sufficiently corrected by spin-echo techniques. The extra transfer operations are a disadvantage, but such a scheme has the benefit that qubits that are not scheduled for gate operations are not as readily dephased by Stark shifts caused by residual stray light from two-qubit gate beams, which are likely to be the most powerful laser beams used in a working QIP device.

Another approach is to use the gate first described by Sørensen and Mølmer [42] and Solano *et al.* [43]. The gate mechanism is basically the same as described above, but in a rotated basis [41], and can be adapted as a transport gate in the more robust way described in Fig. 1(b) of [41]. Here, two counter-propagating beams are offset from the primary beam by $\pm\omega_0$ as shown in Fig. 5. For the proper transport velocity, this would set up a situation equivalent to the one described in [41]. The frequency differences resulting from combining these three Raman beams, including the appropriate Doppler shifts due to the transport, are at $\omega_0 \pm \omega_{\mathrm{str}} + \delta$, creating slow rotating terms near the blue $\omega_0 + \omega_{\mathrm{str}}$ and red $\omega_0 - \omega_{\mathrm{str}}$ sideband transitions in the Hamiltonian (1). This scheme has the advantage that it works for qubits with field-insensitive qubit transition frequencies. However, this comes with some disadvantages. One is the added technical difficulty inherent in creating the frequencies of the required beams. For example, the scheme depicted in Fig. 5 would require acousto-optical modulation at $\omega_0/2$. The smallest value of $\omega_0$ for typically considered hyperfine-state ion qubits is $2\pi \times 1.25$ GHz in $^9Be^+$. Even in this case we would need two specialized modulators at approximately 600 MHz, adding technical complexity. For hyperfine splittings exceeding 2 GHz the modulation would currently require several acousto-optic and/or electro-optic modulators, or a means to offset phase lock of the respective laser beams. Another disadvantage is the relative proximity of the qubit carrier transition at the difference frequency $\omega_0$. To keep perturbations from carrier excitation small, we must use gate durations much longer than $2\pi/\omega_{\mathrm{str}}$. For the $Z$-phase gate described in the preceding sections, the carrier is essentially detuned by $\omega_0$, so gate durations comparable to or shorter than $2\pi/\omega_{\mathrm{COM}}$ could be possible.

Another possible extension consists of fine-tuning the phase-space trajectories with transport patterns featuring nonuniform velocities. Such schemes could lead to better suppression of off-resonant terms and possibly to higher gate speeds. This would probably require numerical modeling, while the simple uniform-velocity transport through Gaussian beams has the appeal that all relevant quantities can be expressed analytically.

More generally the transport gate mechanism can be implemented with any standing wave field that imparts an internal state-dependent force. For example, close proximity of the ions to the trap electrode surfaces should make it possible to set up strong magnetic field gradients to induce state-dependent forces. We could construct a magnetic "washboard" resulting from parallel current-carrying wires with alternating current direction, or strips of permanent magnetic material with alternating polarization oriented perpendicular to the transport direction. As long as the qubit information is contained in states with different energy dependence (slope) as a function of the external field, the field gradients of the washboard produces state-dependent forces. By controlling the transport velocity of the ions we could make them experience these forces in near resonance with a motional mode frequency. Once this situation is established, the gate mechanism is analogous to what has been described in the preceding sections, where the strength and envelope of the alternating force would be given by the particular values of the currents used or the strength of the magnetized strips. Thus a range of envelope functions could be achieved. For example, assume a washboard made of FePt stripes (or domains written into a continuous film) with an alternating magnetization on the order of 800 kA/m, and a period length of $d_m \simeq 20$ $\mu$m could be produced (similar to those of Ref. [44]). As a $^9Be^+$ ion is transported at a height of 17.5 $\mu$m over such a structure at $v_W = 80$ $\mu$m/$\mu$s, this would create a time-dependent magnetic field with an amplitude of

$$B_{\mathrm{tot}}(t) = \sqrt{[B_0 - B_w \cos(\omega_w t)]^2 + [B_w \sin(\omega_w t)]^2}$$
$$\simeq B_0[1 + 1/4(B_w/B_0)^2] - B_w \cos(\omega_w t), \quad (34)$$

with $B_w \simeq 20$ G, $B_0 \simeq 120$ G [45]. This choice of $B_0$ ensures

first-order field independence to a qubit encoded in the $|F=1,m_F=0\rangle$ and $|F=2,m_F=1\rangle$ states in all regions of the array that are sufficiently far from the permanent magnetic elements [40]. To lowest order we have an oscillating field at $\omega_w=2\pi v_w/d_m=4$ MHz that is superimposed on a static average field that is larger than $B_0$ by $B_w^2/(4B_0)\simeq 0.837$ G. We assume that good single-qubit rotations are available to transfer the qubit information into the $|F=2,m_F=-2\rangle/|F=2,m_F=2\rangle$ "stretched" states of the hyperfine manifold. Then, the undulating field of the washboard would lead to a gate Rabi frequency of

$$\Omega_m=\frac{2\pi}{d_m}z_0\frac{\mu_B B_w}{\hbar}\simeq 2\pi\times 73.5 \text{ kHz}, \tag{35}$$

with $\mu_B$ the Bohr magneton and $z_0=\sqrt{\hbar/(4m\omega_{\mathrm{COM}})}$ the extent of the ground-state wave function of the COM mode of two beryllium ions. This Rabi frequency would correspond to a gate duration $\tau_m=\pi/\Omega_m\simeq 6.8$ $\mu$s. At the same time, the slightly higher average field leads to effective single-qubit rotations of about $2\pi\times 15.9$ that commute with the phase gate. These unwanted single-qubit phases could possibly be eliminated by a more sophisticated (symmetrical) geometry of the elements producing the oscillating field, or by dividing the gate into two interactions with washboards that each yield a logical phase of $\pi/4$ and are enclosed in a spin-echo sequence [26].

Gate speeds are limited by the condition that the spins should follow the magnetic field adiabatically. For this to happen, the normalized rate of change of the field $|(d\mathbf{B}/dt)|/B_0$ must be much smaller than the smallest Larmor frequency along the trajectory $\omega_{\min}=\min(\gamma_<|\mathbf{B}|)$, with $\gamma_<$ the smallest gyromagnetic ratio of the states in question and $\mathbf{B}$ the position-dependent magnetic field. The speed of variation of $\mathbf{B}$ is governed by the trap frequency, therefore, at least for a gate utilizing adiabatic following, the gate duration is limited by the trap frequency. The "Lamb-Dicke" parameter that is relevant for this gate is $\eta_m=(2\pi/d_m)z_0$. In contrast to gates mediated by laser fields with wavelengths prescribed by the internal states of the ions, this parameter can be scaled more freely by changing the period length $d_m$ of the microfabricated pattern. Of course the ions must be moved closer to the surface to create a sufficient modulation of the field along their trajectory. This might lead to an increase in anomalous heating, but at the same time the closer proximity of the ions allows use of smaller trap electrodes and scaling the dimensions of the trap array. For gates mediated by light, the need to illuminate ions by laser beams with waists that are most likely limited to sizes of several micrometers from geometrical constraints dictates a minimum distance of the ions to the trap electrodes. This distance in turn governs the minimal electrode dimensions in a trap array. If light is not necessary to mediate the gates we could use trap structures beyond this limit, possibly with stronger confinement of the ions and faster gates.

An additional, but important advantage of such gates is the absence of spontaneous emission that is currently thought to pose the most severe limitation on achievable fidelities for Raman transition gates implemented with laser beams [6].

## IX. SUMMARY AND CONCLUSIONS

Miniaturization of ion traps and scaling up ion-qubit numbers to beyond 10 is now under way in several laboratories. Recent efforts have concentrated on developing technologies for trap arrays compatible with this goal. One of the next steps is to simplify the optics necessary to scale up as much as possible. In this paper we have outlined a few possible techniques toward this goal. Controlled transport of ions is utilized for parallel implementation of quantum logic gates with relaxed requirements for temporal and spatial control of the laser beams. After sketching the basic features of such an architecture based on a multizone trap array, we analyzed one-qubit rotations and a universal two-qubit gate and showed that such gates can be implemented with existing technology.

We also discussed possible extensions of the two-qubit gate mechanism. In particular we sketched one approach that utilizes periodic magnetic field patterns in combination with ion transport to exert state-dependent forces on the ions. This approach might enable more flexible scaling of future trap arrays and could remove some of the limitations to fidelity and gate speed posed by two-qubit gates mediated by laser beams.

## ACKNOWLEDGMENTS

This work was supported by the Disruptive Technology Office under Contract No. 712868, by the Department of Defense Multidisciplinary University Research Initiative (MURI) program administered by the Office of Naval Research and by NIST. The authors thank S. Glancy and T. Rosenband for comments on the paper.

[1] Quantum information science and technology experts panel, 2002, http://qist.lanl.gov/

[2] D. J. Wineland, C. Monroe, W. M. Itano, D. Leibfried, B. E. King, and D. M. Meekhof, J. Res. Natl. Inst. Stand. Technol. **103**, 259 (1998).

[3] D. Kielpinski, C. Monroe, and D. J. Wineland, Nature (London) **417**, 709 (2002).

[4] M. A. Rowe *et al.*, Quantum Inf. Comput. **2**, 257 (2002).

[5] J. Kim, S. Pau, Z. Ma, H. R. McLellan, J. V. Gates, A. Kornblit, R. E. Slusher, R. M. Jopson, I. Kang, and M. Dinu, Quantum Inf. Comput. **5**, 515 (2005).

[6] R. Ozeri *et al.*, Phys. Rev. A **75**, 042329 (2007).

[7] D. P. DiVincenzo, Fortschr. Phys. **48**, 771 (2000).
[8] A. M. Steane, e-print arXiv:quant-ph/0412165.
[9] R. Reichle, D. Leibfried, R. B. Blakestad, J. Britton, J. D. Jost, E. Knill, C. Langer, R. Ozeri, S. Seidelin, and D. J. Wineland, Fortschr. Phys. **54**, 666 (2006).
[10] D. Hucul, M. Yeo, W. K. Hensinger, J. Rabchuk, S. Olmschenk, and C. Monroe, e-print arXiv:quant-ph/0702175.
[11] J. Chiaverini, R. Blakestadt, J. Britton, J. Jost, C. Langer, D. Leibfried, R. Ozeri, and D. J. Wineland, Quantum Inf. Comput. **5**, 419 (2005).
[12] M. D. Barrett *et al.*, Nature (London) **429**, 737 (2004).
[13] C. H. Bennett, G. Brassard, C. Crepeau, R. Jozsa, A. Peres, and W. K. Wootters, Phys. Rev. Lett. **70**, 1895 (1993).
[14] D. Gottesman and I. L. Chuang, Nature (London) **402**, 390 (1999).
[15] M. Riebe *et al.*, Nature (London) **429**, 734 (2004).
[16] E. Knill, Nature (London) **434**, 39 (2005).
[17] A. Barenco, C. H. Bennett, R. Cleve, D. P. DiVincenzo, N. Margolus, P. Shor, T. Sleator, J. A. Smolin, and H. Weinfurter, Phys. Rev. A **52**, 3457 (1995).
[18] C. Monroe, D. M. Meekhof, B. E. King, S. R. Jefferts, W. M. Itano, D. J. Wineland, and P. Gould, Phys. Rev. Lett. **75**, 4011 (1995).
[19] D. Leibfried, R. Blatt, C. Monroe, and D. J. Wineland, Rev. Mod. Phys. **75**, 281 (2003).
[20] D. Wineland *et al.*, Proc. R. Soc. London, Ser. A **361**, 1349 (2003).
[21] H. Kogelnik and T. Li, Appl. Opt. **5**, 1550 (1966).
[22] M. Nielsen and I. L. Chuang, *Quantum Computation and Quantum Information* (Cambridge University Press, Cambridge, UK, 2000).
[23] Both operations are diagonal in the measurement basis.
[24] R. J. Glauber, Phys. Rev. **131**, 2766 (1963).
[25] R. R. Puri, *Mathematical Methods of Quantum Optics* (Springer-Verlag, Berlin, Heidelberg, Germany, 2001).
[26] D. Leibfried *et al.*, Nature (London) **422**, 412 (2003).
[27] M. Sasura and A. M. Steane, Phys. Rev. A **67**, 062318 (2003).
[28] D. Leibfried, M. D. Barrett, T. Schaetz, J. Britton, J. Chiaverini, W. M. Itano, J. D. Jost, C. Langer, and D. J. Wineland, Science **304**, 1476 (2004).
[29] Here we neglect a sign that depends on the value of $n$ and the sign of $\Omega_{\uparrow}-\Omega_{\downarrow}$, but will only determine the orientation of the trajectory in phase space.
[30] H. Rohde, S. Gulde, C. Roos, P. Barton, D. Leibfried, J. Eschner, F. Schmidt-Kaler, and R. Blatt, J. Opt. B: Quantum Semiclassical Opt. **3**, S34 (2001).
[31] B. B. Blinov, L. Deslauriers, P. Lee, M. J. Madsen, R. Miller, and C. Monroe, Phys. Rev. A **65**, 040304(R) (2002).
[32] M. D. Barrett *et al.*, Phys. Rev. A **68**, 042302 (2003).
[33] B. E. King, C. S. Wood, C. J. Myatt, Q. A. Turchette, D. Leibfried, W. M. Itano, C. Monroe, and D. J. Wineland, Phys. Rev. Lett. **81**, 1525 (1998).
[34] A. S. Sørensen and K. Mølmer, Phys. Rev. A **62**, 022311 (2000).
[35] Q. Turchette *et al.*, Phys. Rev. A **61**, 063418 (2000).
[36] L. Deslauriers, P. C. Haljan, P. J. Lee, K.-A. Brickman, B. B. Blinov, M. J. Madsen, and C. Monroe, Phys. Rev. A **70**, 043408 (2004).
[37] L. Deslauriers, S. Olmschenk, D. Stick, W. K. Hensinger, J. Sterk, and C. Monroe, Phys. Rev. Lett. **97**, 103007 (2006).
[38] R. J. Epstein *et al.*, e-print arXiv:quant-ph/0707.1528.
[39] R. Ozeri *et al.*, Phys. Rev. Lett. **95**, 030403 (2005).
[40] C. Langer *et al.*, Phys. Rev. Lett. **95**, 060502 (2005).
[41] P. C. Haljan, K. A. Brickman, L. Deslauriers, P. J. Lee, and C. Monroe, Phys. Rev. Lett. **94**, 153602 (2005).
[42] A. S. Sørensen and K. Mølmer, Phys. Rev. Lett. **82**, 1971 (1999).
[43] E. Solano, R. L. de Matos Filho, and N. Zagury, Phys. Rev. A **59**, R2539 (1999).
[44] Y. Xing, I. Barb, R. Gerritsma, R. Spreeuw, H. Luigjes, Q. Xiao, C. Rétif, and J. Goedkoop, J. Magn. Magn. Mater. **313**, 192 (2007).
[45] E. Hinds and I. Hughes, J. Phys. D **32**, R119 (1999).